N71-31194
NASA TM X-67878

NASA TECHNICAL MEMORANDUM

NASA TM X-67878

ROTATIONAL AND VIBRATIONAL EFFECTS IN ION-DIPOLE COLLISIONS

by John V. Dugan, Jr., Raymond W. Palmer,
and R. Bruce Canright, Jr.
Lewis Research Center
Cleveland, Ohio

TECHNICAL PAPER proposed for presentation at Seventh International Conference on the Physics of Electronic and Atomic Collisions organized under the auspices of the International Union of Pure and Applied Physics (IUPAP) and the Netherlands Physical Society
Amsterdam, the Netherlands, July 25-30, 1971

ABSTRACT

This paper consists of a motion picture script supplemented by eight figures. This script is the sound track for a 17-minute (16-mm) color motion picture. This motion picture film supplement C-275 is available on loan.

The film consists of five separate computer-made collision sequences, five animated sequences and eight stills, some of which are computer-made time history plots. The behavior of ion-dipole collisions is contrasted with ion-induced-dipole (Langevin) collisions.

Film supplement C-275 is available on request to:

Chief, Management Services Division (5-5)
National Aeronautics and Space Administration
Lewis Research Center
21000 Brookpark Road
Cleveland, Ohio 44135

E-6445

ROTATIONAL AND VIBRATIONAL EFFECTS IN ION-DIPOLE COLLISIONS

by John V. Dugan, Jr., Raymond W. Palmer, and R. Bruce Canright, Jr.

National Aeronautics and Space Administration
Lewis Research Center
Cleveland, Ohio

INTRODUCTION

This paper consists of a motion picture script supplemented by eight figures. This script is the sound track for a 17-minute (16-mm) color motion picture. This motion picture film supplement C-275 is available on loan.

The film consists of five separate computer-made collision sequences and eight stills, some of which are computer-made time history plots. The behavior of ion-dipole collisions is contrasted with ion-induced-dipole (Langevin) collisions.

Ion-molecule interaction potentials are significant at large separations where neutral-molecule potentials are negligible. Ion trajectories in the field of an induced dipole were studied by Langevin. The potential is:

$$V(R) = -\frac{\alpha e^2}{2R^4}$$

where alpha and e are the electronic polarizability and charge and R is the ion-molecule separation. The capture cross section for such orbits is:

$$\sigma_L = \pi b_L^2$$

the critical impact parameter is:

$$b_L = \left(\frac{2\alpha e^2}{\varepsilon}\right)^{1/4}$$

where epsilon is the relative translational energy at infinite separation. For b less than b_L capture always occurs. All trajectories with b greater than b_L are simple scatterings.

Many molecules have permanent electric dipole moments. The corresponding potential expression has the terms

$$-\mu e \frac{\cos \gamma}{R^2} + \frac{-\alpha e^2}{2R^4}$$

where gamma is the ion-dipole orientation angle. A molecule with a permanent dipole moment cannot be treated as a point particle since the interaction potential is a function of rotational energy. This movie summarizes some of the results of trajectory calculations done by the authors; the early work was done in collaboration with Professor John L. Magee of the University of Notre Dame.

One limiting case is that of a polar molecule with zero moment of inertia colliding with an ion. In this case, the dipole can adjust its orientation as the collision develops, the angle gamma is always zero and the largest possible cross section results. This maximum cross section is:

$$\sigma_M \equiv \pi b_M^2 = \pi\left\{\frac{\mu e}{\varepsilon} + \left(\frac{2\alpha e^2}{\varepsilon}\right)^{1/2}\right\}$$

This limiting case is termed "adiabatic" i.e. the completely hindered case, because the dipole alines itself with the ion throughout the collision.

Another limiting case is the very energetic rotator which is unaffected by the ion, i.e., the completely unhindered case. Averaging over all possible orientations gives a lower limit cross section.

$$\sigma_\gamma \equiv \pi b_\gamma^2 = \pi\left\{\frac{\mu e}{4\varepsilon}\left(1 - \frac{2\alpha\varepsilon}{\mu^2}\right) + \left(\frac{\alpha e^2}{2\varepsilon}\right)^{1/2} + \left(\frac{\alpha e}{\mu}\right)\right\}$$

Calculations have been done which are based on a classical model for the ion-molecule collision. The potential energy includes both ion-dipole and ion-polarizability terms for capture cross section calculations. In all cases the structureless ion enters only through its charge and mass.

The coordinate system used for the calculations involving linear polar molecules is shown in Fig. 1. The center-of-mass of the ion and molecule and the ion-dipole orientation angle gamma are indicated. Trajectories were calculated for many impact parameters at different ion velocities and target rotational temperatures. For an initial energy and impact parameter, there is a probability that the system will arrive at an ion-molecule separation corresponding to capture. The fraction of collisions having this result we call the "capture ratio" C sub R.

The Langevin trajectories have a simple property; the "all-or-

nothing" capture ratio is a step function. The derivation of the maximum cross section for a polar molecule assumes that these collisions are also all-or-nothing situations. The calculated ion-dipole collisions do <u>not</u> have this property.

A plot of capture ratio (for the methyl cyanide parent-ion system) against impact parameter is shown in Fig. 2 for an ion velocity of 5 times 10^4 centimeters per second and rotational temperatures of 300 and 77 degrees Kelvin. The ratios are shown for Langevin b_L the maximum b_M and the limiting b_γ. The dipole does not exert its maximum effect in causing capture and sometimes prevents capture as C_R falls below unity for b less than b_L. But, the very large dipole effect on capture is clear from comparison with Langevin values. Polarization of the rotor brings about an orientation with the field and the capture ratio should increase as the average rotational energy decreases. Thus, C_R is larger at the lower temperature. The "capture collision" cross section is

$$\sigma_c \equiv \pi \int_0^{b_0} C_R(b^2)\,d(b^2)$$

where b_0 is the impact parameter at which C_R becomes zero. A comparison with results of methyl cyanide experiments is presented in Fig. 3 and shows satisfactory agreement.

Examination of the calculated trajectories indicates that there is very rapid energy exchange between translational and rotational modes. This energy transfer can lead to formation of long-lived collision complexes via multiple reflection behavior.

We choose to approximate short-range interactions by a hard inner core potential ϕ_c, with a radius R_c of 3 angstroms where the potential energy rises to infinity.

A plot of effective potential shown in Fig. 4 illustrates the multiple-reflection mechanism. The effective potential consists of the interaction and angular momentum terms. In the Langevin case, the ion starts at infinity with translational energy ϵ_1, goes over the barrier at R^*, reflects off ϕ_c and returns to large R. In the dipole target case the barrier height is a function of dipole orientation. Thus the ion goes over the barrier at R' before reflection as the dipole barely rotates. However, as reflection occurs, the dipole alters its orientation, erecting higher barrier at R''. The translational energy is now insufficient for the ion to escape and another reflection occurs.

Thus, in the Langevin case, simple specular reflection occurs, whereas the rotating dipole introduces outer turning points and multiple reflections result.

Relative speed and rotational energy are shown versus separation in Fig. 5 for a single reflection collision with a methyl cyanide target. The velocity increases with decreasing R until the potential energy becomes a minimum. The rotational energy changes drastically. Variations of the outer turning points for methyl cyanide targets with net spiraling of collision partners are shown (Fig. 6).

These computer-plotter studies have included making motion pictures of ion-polar-molecule collisions. Each motion picture (see Fig. 7) frame shows the projection of ion and molecule in a plane through the center-of-mass of the pair. The ion is represented by a disk. The molecular dipole is a dumbbell with disks at each end. The molecule consists of the dipole surrounded by a circle of triangles. The radii of the circle and disks are varied above and below the plane.

The first collision involving a methyl cyanide molecule and ion is a single-reflection collision. The methyl cyanide molecule rotates rapidly until the particles come within 10 angstroms of each other; then it becomes hindered. This is a head-on reflection, followed by mutual spiraling of the ion and molecule, and differs from the simple specular Langevin reflection. The dipole is strongly hindered throughout the interaction because the ion-dipole potential term is quite large. The molecule departs above the plane with the ion below it.

The second sequence shows a 10-reflection methyl-cyanide parent-ion collision with the molecule approaching slightly below the plane. An interesting aspect of this collision is the mutual spiraling of partners at distances of about 15 angstroms corresponding to a large characteristic radius for the ion-molecule complex. Radii as large as 20 to 23 angstroms have been observed for the methyl-cyanide system. (This is in contrast to the carbon-monoxide system where the radii are characteristically 3 to 5 angstroms.) There is pronounced spiraling at large distances for methyl-cyanide, and this occurs because there is a large dipole moment. The dipole momentarily becomes dramatically hindered, and its angular momentum is converted to the mutual spiraling motion.

In hydrochloric acid collisions, the average number of reflections in a multiple-relfection collision is high, but their occurrence is rare. This is because of the small moment of inertia of hydrochloric acid. The combination of large moment of inertia and large dipole moment for methyl cyanide causes multiple-reflection behavior to be highly probable.

Presumably, molecular vibration will affect both the capture cross section and the extent of energy transfer.

Vibration is incorporated in the collision model by making the semi-classical assumption that the dipole moment is a function of instantaneous molecular bond length r. The vibrator coordinate x

is defined as the instantaneous displacement of the bond from its equilibrium length r sub e (see Fig. 6). The instantaneous dipole moment is assumed gaussian

$$\mu(x) = \mu_0 e^{-a^2x^2}$$

where mu sub zero is the "static" mu value and a is a molecular constant. Two sets of vibrators were studied; with mu of x a weak function of displacement, set (A), and strong function, set (B).

A sample vibrator movie frame is shown (see Fig. 9). The dipole length is now variable. The vertical marks at the top indicate the inner turning point, the x equals zero point and outer turning point of the free vibrator. An ellipse at the top of the frame marks the instantaneous x value and magnifies the vibrator extension (x greater than zero) or compression (x less than zero). The total energy of the free vibrator is

$$E_0 = m_0x^2/2 + k_0x^2/2$$

where m sub zero is the oscillator mass and k sub zero is the force constant equal to 50 Newtons per meter.

The nature of the multiple reflection behavior is generally unchanged by the molecular vibration. However, the mode of vibration is affected dramatically by the dipole field.

The differential equation of motion for the molecular vibration along the polar bond is

$$\ddot{x} = -(2a^2\mu e \cos\gamma/R^2 + k_0)x/m_0$$

The first term is the ion-dipole interaction; the second is the conventional restoring force.

The collision lifetimes are relatively insensitive to vibrations; however, the capture ratio depends strongly on the value of the constant a.

The first ion-molecule collision including vibration, involves a target with a weak mu of x variation which behaves very much like a purely rotating target. This sequence demonstrates simple modulation of the vibrator amplitude by the ion-dipole interaction during a multiple reflection collision. The amplitude of the oscillation decreases with some increase in frequency at smaller R values. One glancing reflection occurs at a small ion-molecule separation as the amplitude

remains somewhat less than that of a free vibrator. Nine additional reflections occur after some mutual spiraling at large separations accompanied by considerable vibrational and rotational excitation.

A change in mode occurs when the vibrator acceleration remains near zero for a significant fraction of a vibrational period. The constraining of the vibrator so that it cannot relax to its equilibrium separation is somewhat analogous to quantum mechanical tunneling through a potential barrier. Thus, we have chosen to call it "classical tunneling." The time history plots of vibrator displacement x and velocity x dot in Fig. 10 show that the acceleration x double dot stays near zero for a significant fraction of a vibrational period (where x dot is nearly constant). All tunneling is observed when gamma is slightly greater than ninety degrees so cosine gamma is very small and negative.

The second collision sequence demonstrates classical tunneling after the vibrator is first modulated. As the orientation angle approaches ninety degrees the amplitude of vibration approaches that of a free vibrator; however, the energy is increased. When gamma passes through pi over two "tunneling" occurs, the vibrator translates to vibrate near the outer turning point. The vibrator returns to its conventional mode when gamma passes back through pi over two. The ion and molecule are approaching for further reflections as the sequence ends.

The third sequence is interesting from two standpoints. Multiple tunneling occurs, and tunneling takes place at large separations. The nearly free vibrator shifts to the inner turning point and returns to its oscillation about x = 0 as the dipole tumbles end over end. There is another tunneling at a separation of 5 angstroms as the constrained vibrator increases amplitude and then becomes compressed.

The vibrator returns to the conventional mode as the first reflection occurs and then tunnels into the extended mode. During the second reflection the vibrator returns to its conventional mode as the dipole becomes extremely hindered. While the collision partners continue to orbit, there is a third reflection which is accompanied by a fourth compressed tunneling. As the particles retreat from each other, the vibrator returns to its free mode at roughly 15 angstroms.

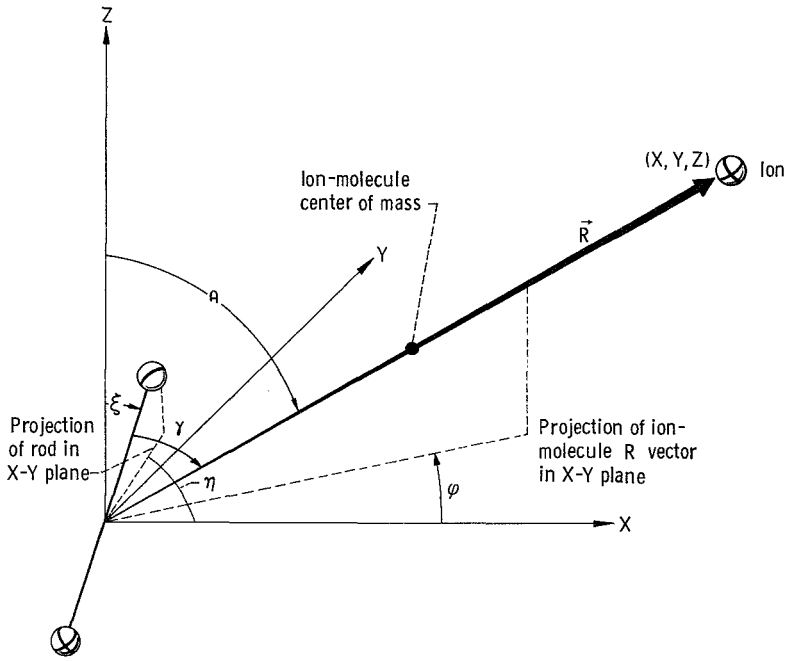

Figure 1. - Coordinate system used in computer study of interaction between an ion and linear polar molecule.

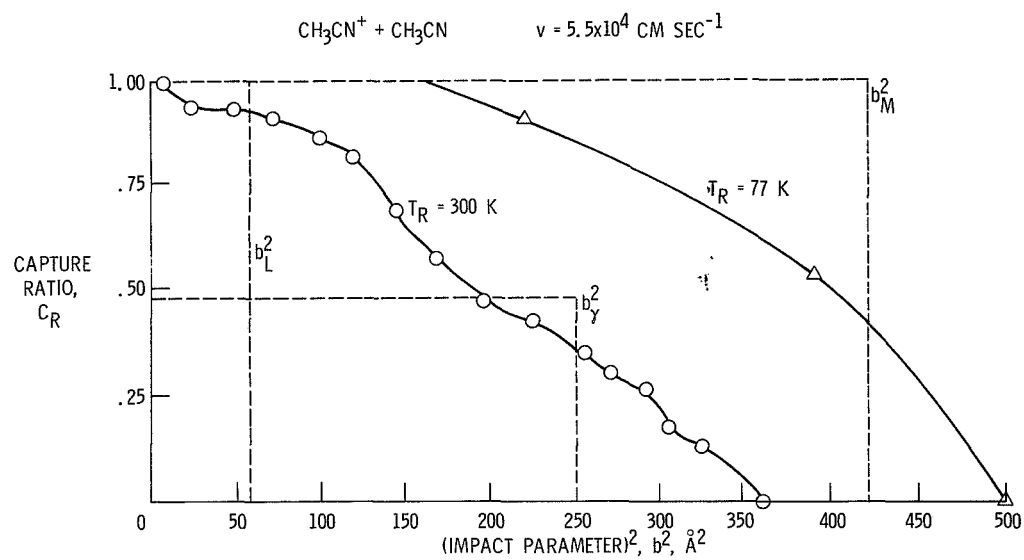

Figure 2. - Variation of capture ratio with impact parameter for target rotators chosen from heat baths at 77 and 300 K composed with Langevin and completely unhindered and hindered limiting cases.

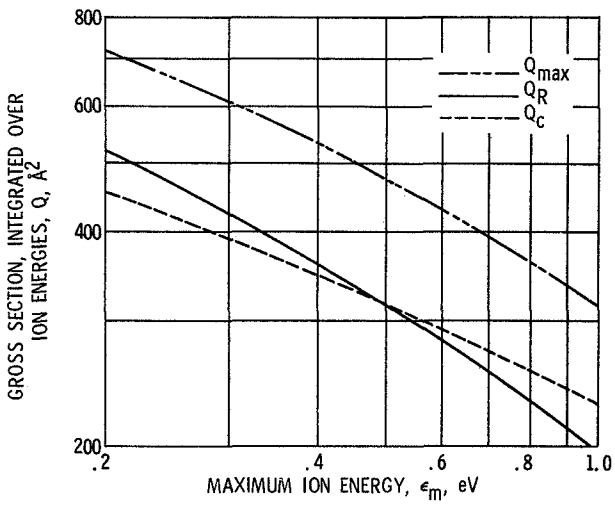

Figure 3. - Comparison of numerical capture cross section Q_c with experimentally assumed capture cross section Q_{max} and observed reaction cross section for methyl cyanide-parent ion collision as function of maximum ion energy ϵ_m.

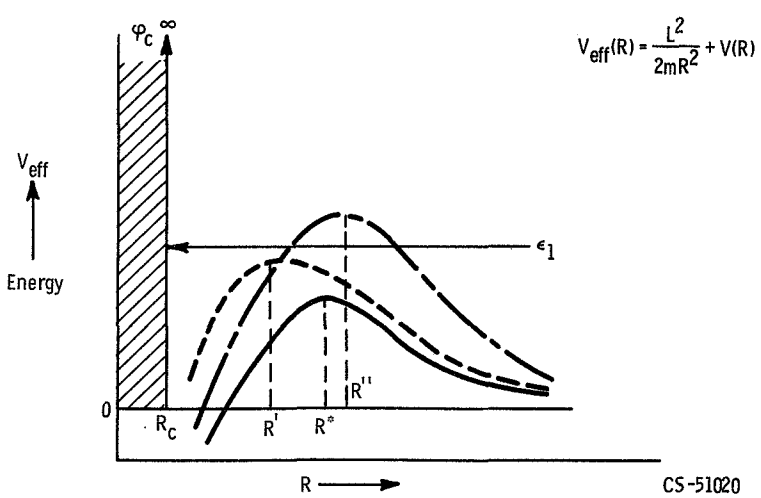

Figure 4. - Schematic diagram illustrating mechanism of multiple reflection phenomena in ion-dipole collisions with plots of effective potentials for Langevin and permanent dipole collision systems against ion-molecule separation.

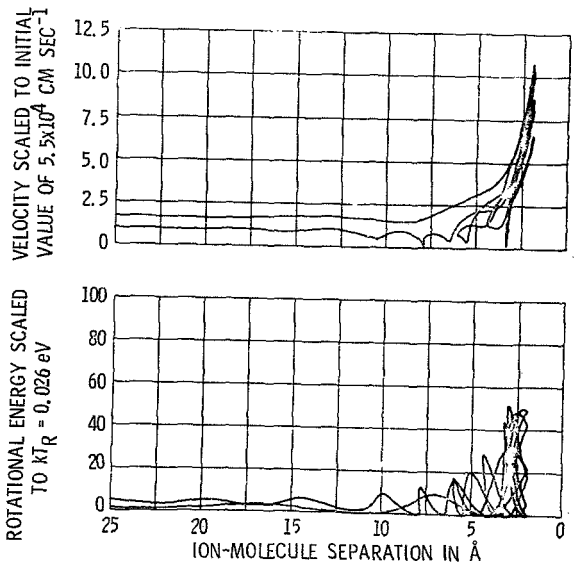

Figure 5. - Variation of ion velocity and polar molecule rotational energy during methyl cyanide-parent-ion multiple reflection capture collision.

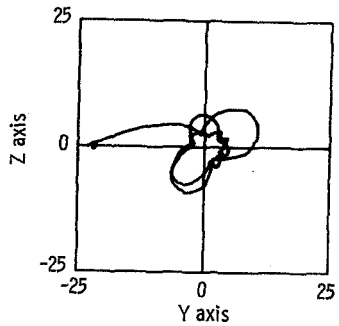

Figure 6. - Projection of ion trajectory in Y-Z plane of cartesian coordinate system with origin at cm of CH_3CN molecule.

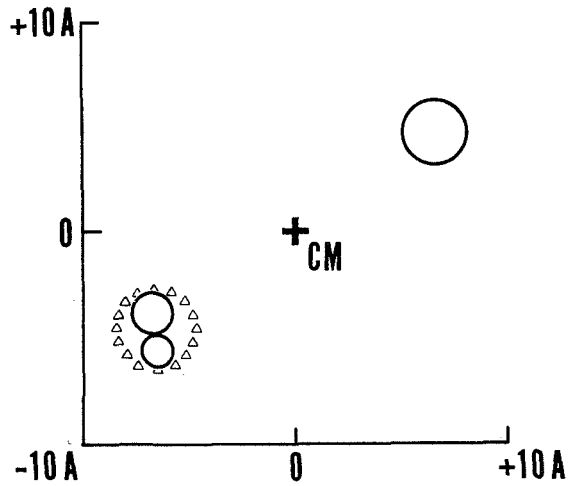

Figure 7. - Sample movie frame for ion-dipole studies with rotating target showing polar molecule and ion projections in 20x20 Å plane of the center-of-mass system.

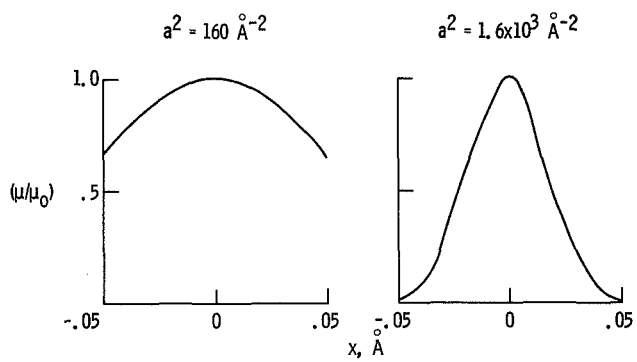

Figure 8. - Dipole moment variation for polar target oscillators studied sets (A) and (B), $|x_m|_0$ = 0.05 Å; $\mu = \mu_0 \exp\left[-a^2x^2\right]$.

I . 0 I

Figure 9. - Sample movie frame for ion-dipole studies with vibrating-rotating target showing extended molecular vibrator and ion projections in plane of the center-of-mass system.

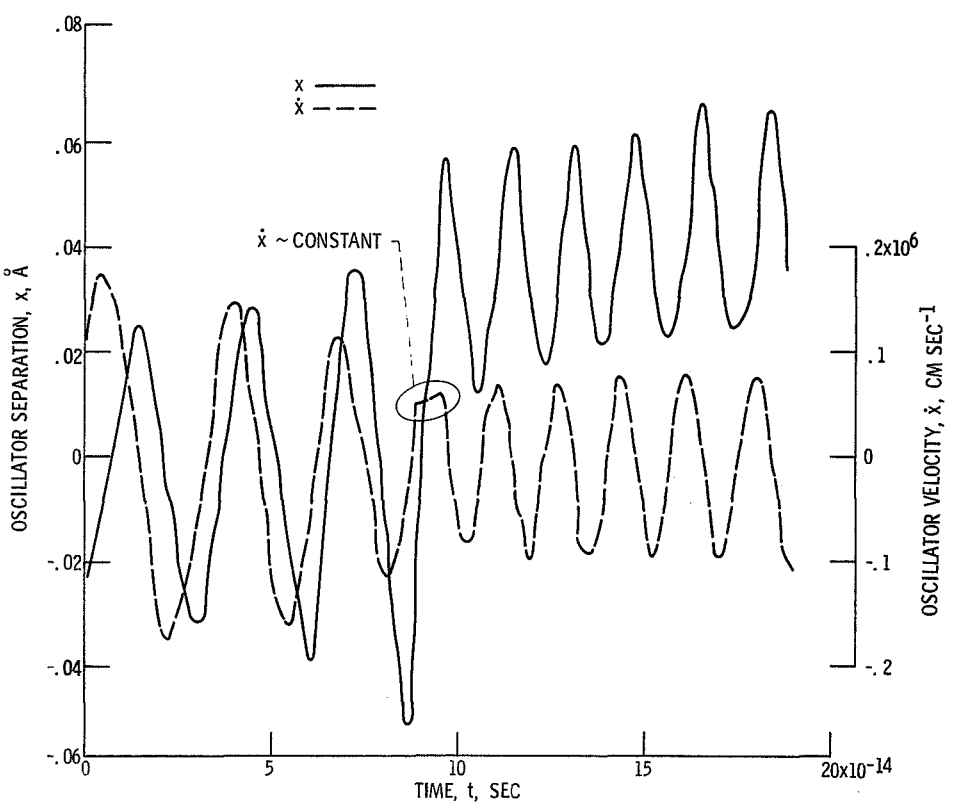

Figure 10. - Variations of oscillator separation and velocity for ion-dipole collision demonstrating "classical tunneling."

NASA-Lewis-Com'l